

**UNIVERSIDAD SAN FRANCISCO DE QUITO
USFQ**

Colegio de Ciencias e Ingenierías

**Seismic Response Analysis of a Layered Soil Column Under
Different Water Conditions**

Diego Antonio Camacho Davalos

Ingeniería Civil

Trabajo de fin de carrera presentado como requisito
para la obtención del título de
Ingeniería Civil

Quito, 9 de diciembre de 2021

**UNIVERSIDAD SAN FRANCISCO DE QUITO
USFQ**

Colegio de Ciencias e Ingenierías

**HOJA DE CALIFICACIÓN
DE TRABAJO DE FIN DE CARRERA**

**Seismic Response Analysis of a Layered Soil Column Under
Different Water Conditions**

Diego Antonio Camacho Davalos

**Nombre del profesor, Título académico
Vial**

Juan Pablo Villacreses, Msc, Ing.

Quito, 9 de diciembre de 2021

© DERECHOS DE AUTOR

Por medio del presente documento certifico que he leído todas las Políticas y Manuales de la Universidad San Francisco de Quito USFQ, incluyendo la Política de Propiedad Intelectual USFQ, y estoy de acuerdo con su contenido, por lo que los derechos de propiedad intelectual del presente trabajo quedan sujetos a lo dispuesto en esas Políticas.

Asimismo, autorizo a la USFQ para que realice la digitalización y publicación de este trabajo en el repositorio virtual, de conformidad a lo dispuesto en la Ley Orgánica de Educación Superior del Ecuador.

Nombres y apellidos: Diego Antonio Camacho Davalos

Código: 00200892

Cédula de identidad: 1721780524

Lugar y fecha: Quito, 7 de diciembre de 2021

ACLARACIÓN PARA PUBLICACIÓN

Nota: El presente trabajo, en su totalidad o cualquiera de sus partes, no debe ser considerado como una publicación, incluso a pesar de estar disponible sin restricciones a través de un repositorio institucional. Esta declaración se alinea con las prácticas y recomendaciones presentadas por el Committee on Publication Ethics COPE descritas por Barbour et al. (2017) Discussion document on best practice for issues around theses publishing, disponible en <http://bit.ly/COPETHeses>.

UNPUBLISHED DOCUMENT

Note: The following capstone project is available through Universidad San Francisco de Quito USFQ institutional repository. Nonetheless, this project – in whole or in part – should not be considered a publication. This statement follows the recommendations presented by the Committee on Publication Ethics COPE described by Barbour et al. (2017) Discussion document on best practice for issues around theses publishing available on <http://bit.ly/COPETHeses>.

TABLA DE CONTENIDOS

Resumen	6
Abstract.....	8
Introduction	9
1. Materials.....	11
1.1 Material properties.....	11
1.2 Water retention curve (WRC).....	12
2. Methods	13
2.1 Rheometer.....	13
2.2 Climatic Chamber.....	13
2.3 Finite difference model.....	14
2.4 Finite Element model for site response analysis of soil deposit.....	15
2.4.1 Model description.....	15
2.4.2 Soil Material Properties.....	16
2.4.2.1 Poisson Ratio	16
2.4.2.2 Soil Shear Wave Velocity.....	17
2.4.2.3 Effective stress.....	17
2.4.3 Seismic Motion.....	18
3. Results and discussion.....	19
3.1 Material properties (climate chamber, rheometer).....	19
3.2 Finite-difference simulation (water table level and evaporation).....	22
3.3 Seismic response.....	25
Conclusions	30
References	32

INDICE DE TABLAS Y FIGURAS

Table 2. Soil Properties	11
Figure 1. Particle size distribution.....	12
Figure 2. (WRC) Water retention curve [2].	13
Figure 3. Visual representation of finite element site response model. [3].....	16
Figure 4. Applied ground motion acceleration and Fast Fourier Transform for a) 1989 Loma Prieta earthquake Gilroy N°1 E-W station b) amplified 1995 Kobe earthquake and c) amplified 1989 Loma Prieta earthquake Piedmont	19
Figure 5. Degree of saturation as a function of bulk density.....	20
Figure 6. relationship between the shear modulus (G) and the effective stress (σ').	21
Figure 7. Modulus reduction curves for multiple suction pressure values.....	22
Figure 8. relationship between the degree of saturation (Sr), bulk density (γ_b), water pressure (Uw), and depth of soil deposit (H) for 0, 600, and 87600 hours of the evaporation process and water table levels of a)5m b)15m and c)25m.....	23
Figure 9. relationship between a) shear modulus and depth for different water table levels and b) shear wave velocity and depth for different water table levels for 0, 600, and 87600 hours of the evaporation process	25
Figure 10. 1995 Kobe earthquake acceleration response spectrum at top of the deposit for different water table levels (i.e., 5, 15, 25m) and exposed to 0 and 87600 hours of evaporation	27
Figure 11. 1989 Loma Prieta (Piedmont station) acceleration response spectrum at top of the deposit for different water table levels (i.e., 5, 15, 25m) and exposed to 0 and 87600 hours of evaporation	28
Figure 12. 1989 Loma Prieta (Gilroy N°1 E-W) acceleration response spectrum at top of the deposit for different water table levels (i.e., 5, 15, 25m) and exposed to 0 and 87600 hours of evaporation	30

Resumen

Los efectos de sitio sísmicos se ven afectados por las propiedades mecánicas y dinámicas del suelo. Estas propiedades se ven influenciadas por la cantidad de agua que posea el suelo y esta cantidad depende de las condiciones climáticas a las que esté expuesto el suelo. Este trabajo tiene como objetivo realizar un análisis de sitio sísmico en una columna de suelo de treinta metros. Esta columna estará sometida a diferentes niveles freáticos y múltiples periodos de evaporación. Las propiedades mecánicas del suelo ante diferentes valores de succión fueron obtenidas de (Villacreses, Granados, Caicedo, Torres-Rodas, & Yépez, 2021) y (Villacreses, Caicedo, Caro, & Yépez, 2020). Posteriormente, un modelo de diferencias finitas fue aplicado para simular la interacción suelo-ambiente y los resultados fueron utilizados para construir los perfiles de agua de la columna. Finalmente, se modificó un modelo de elementos finitos para simular la respuesta sísmica en la superficie de la columna (McGann & Arduino, 2010). Para esta investigación se utilizaron tres señales sísmicas: el sismo de 1989 en Loma Prieta estación Gilroy N°1 E-W, el sismo de 1995 Kobe amplificado y el sismo de 1989 en Loma Prieta estación Piedmont amplificado. Esta investigación demostró diferencias significativas en la respuesta sísmica en superficie en dependencia del grado de saturación de la columna. Los resultados demostraron que, para las señales estudiadas, los efectos de evaporación no producen un cambio significativo en la respuesta sísmica en superficie. Por el contrario, los resultados demostraron que la posición del nivel freático, si produce diferencia significativa en la respuesta sísmica en superficie. En este estudio se muestra que el depósito en condiciones más secas produce una respuesta de aceleración mayor al depósito en condiciones más saturadas. Este trabajo abre puertas a nuevas investigaciones en las que se estudie el efecto de la posición del nivel freático y los cambios climáticos en las propiedades mecánicas y dinámicas del suelo. Estas

investigaciones pueden ser de utilidad para un mejor entendimiento del comportamiento del suelo Además sería de gran importancia para prevenir pérdidas materiales y sobre todo de vidas humanas ante futuras actividades sísmicas.

Palabras clave: Efectos de sitio sísmico, módulo de corte, acelerograma, nivel freático.

Abstract

The seismic site effect is influenced by the soil's mechanical and dynamical properties. These properties are affected by the water content of the soil, which varies according to the climate conditions to which it is exposed. This work aims to analyze the seismic site effect of a thirty-meter soil column. The column will be submitted to different water table levels and evaporation periods. The mechanical properties under different suction pressures were obtained from (Villacreses, Granados, Caicedo, Torres-Rodas, & Yépez, 2021) and (Villacreses, Caicedo, Caro, & Yépez, 2020). Then, a finite-difference model was used to simulate the soil-environment interaction and the results were applied to build the water profiles of the column (Villacreses, Granados, Caicedo, Torres-Rodas, & Yépez, 2021). Finally, a finite element model was modified to simulate the seismic response at the top of the deposit (McGann & Arduino, 2010). Also, this investigation analyzed the response of three seismic motions: the 1989 Loma Prieta earthquake at Gilroy N°1 E-W station, the amplified 1995 Kobe earthquake, and the amplified 1989 Loma Prieta earthquake in Piedmont. This investigation showed a remarkable difference in soil response according to the degree of saturation of the column. The results showed that, for the studied records, climate conditions do not have a significant effect on the seismic response of the column. On the contrary, the results showed that the water table level can have a significant change in the amplification response of the signal. In this study, the results showed that the deposit with dryer conditions had a greater response acceleration in the surface than deposit in a wetter state. This work opens many research possibilities, where the influence of water content and climate conditions in soil mechanical and dynamical properties can be studied. These investigations would help achieve a better understanding of soil behavior. It

could also be of great significance to help in the prevention of material and moreover human losses due to seismic activity.

Key words: Seismic site effect, shear modulus, accelerogram, water table level.

Introduction

The seismic site effect is strongly affected by the geological conditions of the location. Concerns about seismic wave propagation have increased because of many natural disasters over the last decades. The 1985 Mexico City earthquake is a perfect example of site amplification. This earthquake produced at least 5,000 casualties and many structural damages because of seismic amplification in clay layers and thick sediments. After this unprecedented event, earthquake engineers recognized the importance of understanding local amplification to prevent human and material damages (Sánchez Sesma, Rodríguez Zúñiga, Pérez Rocha, Cuevas, & Suarez, 1992).

The modeling and understanding of the seismic site effect have had a significant development in the past decades. Research has focused on modeling soil properties and more realistic configurations. These analyses, commonly use damping, soil density, and dynamic properties (i.e., shear modulus) as their main inputs to describe the seismic site effect. Nevertheless, soil properties are not uniform, and studies suggest that changing water content has a significant effect on soil dynamic resistance. To support this idea, Villacreses et al. state that the structural stiffness of a soil structure changes due to the water pressure inside de soil skeleton (Villacreses, Granados, Caicedo, Torres-Rodas, & Yépez, 2021). Furthermore, climatic conditions can alter water content in the soil structures. To the best of the author's knowledge, there is little research that considers different water contents and changing properties due to climate conditions in seismic site effect. Therefore, this investigation is the first approximation to a better

understanding of the influence of water content and changing climate conditions in seismic response analysis.

In this investigation, the seismic response analysis of a layered soil column will be assessed. Two factors will be analyzed as parameters that affect seismic response analysis: water table level and changing climate conditions expressed in terms of evaporation. To achieve this objective, the material properties of the soil at different suction pressure values were obtained from the literature (Villacreses, Granados, Caicedo, Torres-Rodas, & Yépez, 2021) and (Villacreses, Caicedo, Caro, & Yépez, 2020). Then, a finite difference model from (Villacreses, Granados, Caicedo, Torres-Rodas, & Yépez, 2021) was used to simulate changing climate conditions. Finally, a finite element model from (McGann & Arduino, 2010) was modified to assess the seismic wave propagation along the soil strata.

1. Materials.

1.1 Material properties

This investigation assesses an idealized soil deposit of fine-grained kaolin. The soil properties, shown in Table 1, were determined in (Villacreses, Caicedo, Caro, & Yépez, 2020) and (Villacreses, Granados, Caicedo, Torres-Rodas, & Yépez, 2021). The soil was classified using the Unified Soil Classification System (USCS) as a high plasticity clay (C.H). Additionally, the Soil Atterberg Limits are a plasticity index of 56%, a liquid limit of 87%, and a plastic limit of 37%. Figure 1 shows the grain size distribution of the studied material. The soil has a well-graded granulometry, with a uniformity coefficient of 3.8 and percentile values D_{30} , D_{50} , and D_{90} of $1.5\mu\text{m}$, $2.5\mu\text{m}$ and $9\mu\text{m}$, respectively. The dry density of the material is 1.35 g/cm^3 and a water content of 31.3%. The properties are summarized in Table 1.

<i>Plastic Limit (%)</i>	87
<i>Liquid Limit (%)</i>	37
<i>Water Content (%)</i>	31.3
<i>Dry Density (g/cm^3)</i>	1.35
<i>D_{30} (μm)</i>	1.5
<i>D_{50} (μm)</i>	2.5
<i>D_{90} (μm)</i>	9

Table 1. Soil Properties

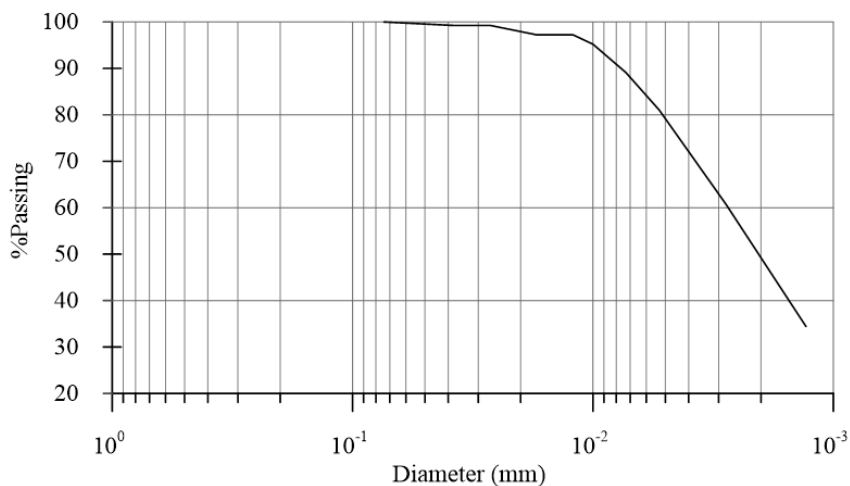


Figure 1. Particle size distribution

1.2 Water retention curve (WRC)

The mechanical properties of soil can have a difference according to the degree of saturation. For this reason, it is pertinent to study the relationship between the water retention curve and the elastic properties. The conducted process was described meticulously in (Villacreses, Caicedo, Caro, & Yépez, 2020). This methodology consisted in measuring the shear modulus on conditioned samples exposed to a relative humidity of 52.4%. The test was finished when the sample reaches the residual water content of 3%. A chilled mirror hygrometer was used to measure the suction pressure (ψ), and the degree of saturation (S_r) was computed using the specific gravity of the soil and the volumetric information of the samples throughout the conditioning process (Leong, Tripathy, & Rahardjo, 2003). Figure 2 shows the water retention curve of the soil material which was obtained from the investigation conducted in (Villacreses, Caicedo, Caro, & Yépez, 2020). In the figure, the soil's suction increases from 10^3 KPa to 10^4 KPa when the degree of saturation decreases from 70% to 20%. The change of soil's suction affects the effective stress and consequently the modulus of the material.

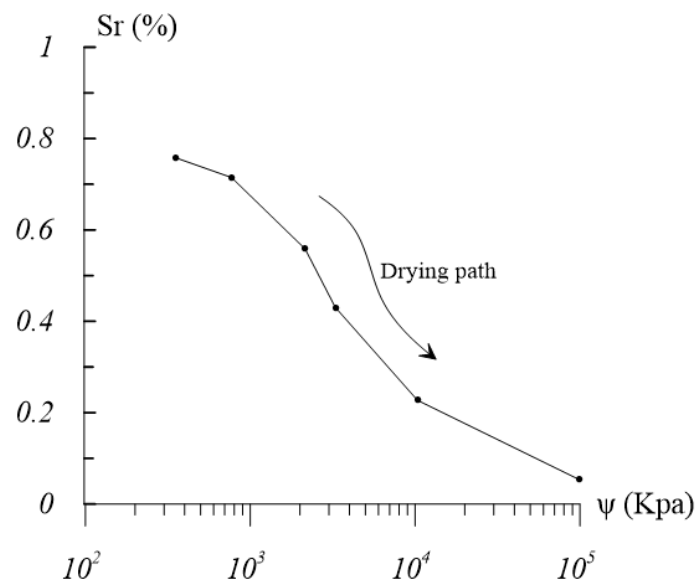


Figure 2. (WRC) Water retention curve (Villacreses, Caicedo, Caro, & Yépez, 2020).

2. Methods

The following section provides the methodologies used in this investigation. The gathered information and data collection from (Villacreses, Caicedo, Caro, & Yépez, 2020), (Villacreses, Granados, Caicedo, Torres-Rodas, & Yépez, 2021), and (Lysmer & Kuhlemeyer, 1969) are presented. Also, the section provides the procedure used to simulate water evaporation and the model used for site response analysis of soil deposits.

2.1 Rheometer

The mechanical properties of the soil subjected to different degrees of saturation were used in a numerical simulation. The simulation seeks to evaluate the performance of a soil deposit under changing weather conditions. Villacreses et al. presented an experimental procedure to determine dynamic shear modulus and damping coefficients using a Torsional Dynamic Shear Rheometer. The procedure, described in (Villacreses, Granados, Caicedo, Torres-Rodas, & Yépez, 2021), uses cylindrical 1.3cm diameter soil specimens, with a 4.0cm height. The samples are conditioned to a controlled relative humidity using the air-drying technique. Finally, the sample's base is fixed, and the top is subjected to a sinusoidal torsional loading scheme. Suction is measured after every torsional test, applying the hygrometer method described in (Villacreses, Caicedo, Caro, & Yépez, 2020) and (Leong, Tripathy, & Rahardjo, 2003).

2.2 Climatic Chamber

Soil's water content and its mechanical properties are directly influenced by changing weather conditions. To study these climate effects on soil's water content, Lozada et al. designed a climatic chamber. This instrument is capable of simulating variables such as wind velocity, solar irradiance, atmospheric pressure, and relative

humidity (Lozada, Caicedo, & Thorel, 2019). In this investigation, soil samples were subjected to different conditions, and the chamber's digital scale allowed water evaporation rates to be determined. These evaporation rates were used to estimate the soil's water content evolution during a drying process.

2.3 Finite difference model

The mechanical properties of the soil are obtained in section 2.1. The water flux behavior is achieved from section 2.2. Once obtained these results, a finite difference simulation is used to compute the soil drying and wetting (Villacreses, Granados, Caicedo, Torres-Rodas, & Yépez, 2021). This model is used to obtain various water content profiles. The model considered two assumptions: porosity is constant over time and flow in the vapor phase is neglected. The model used the continuity equation of water flow in unsaturated soils, given in Eq. (1)

$$n \frac{\partial S_r}{\partial t} + \nabla \cdot (-k_w(S_r) \nabla \psi) = 0 \quad (1)$$

Where (S_r) represents the degree of saturation, (t) time, (n) soil's porosity, (ψ) total potential and (k_w) water conductivity of the liquid phase. Then, a forward difference time operator and the central difference two-dimensional space operator in Eq. (1) permitted a time and space domain discretization. Thus, discretized continuity equation allowed the construction of Eq. (2) which describes the evolution of soil's total potential in time. A complete explanation of the mathematical approach is shown in (Villacreses, Granados, Caicedo, Torres-Rodas, & Yépez, 2021).

$$n \frac{\partial S_r}{\partial t} = C_\theta \frac{\partial s}{\partial t} = C_\theta \frac{\psi_{i,j}^{t+\Delta t} - \psi_{i,j}^t}{\Delta t} \quad (2)$$

2.4 Finite Element model for site response analysis of soil deposit

2.4.1 Model description

A finite element simulation is used to analyze the seismic response of a soil deposit. The model used in this work was obtained from an investigation conducted by McGann & Arduino (McGann & Arduino, 2010). This model computes the reaction of a one-dimensional soil column which is divided into layers. The finite element model uses a Pressure Independent Multi-yield material to simulate the behavior of undrained clays. The column is subjected to an earthquake ground motion to compute the surface response.

The simulation computes the seismic response for a 30 meters depth soil deposit. This depth was selected because most of the Ecuadorian regulations establish geotechnical exploration to this depth for seismic analysis (MIDUVI, 2014). The soil deposit profile is divided into thirty layers of one meter each. This deposit is settled in a bedrock. The simulated bedrock has a shear wave velocity of 1524 m/s. The model implements Lysmer-Kuhlemeyer's dashpot at the base of the soil profile, explained profoundly in (McGann & Arduino, 2010) and (Lysmer & Kuhlemeyer, 1969). Figure 3 shows the mesh and nodes geometry used for the model. The figure shows that for n elements, there are $2n+1$ nodes. These nodes are numbered by a left-to-right, top-to-bottom system. Nodes 1 and 2 nodes are fixed against y -direction displacements. Nodes from node 3 to node $2n+2$ are tied together using an equal degree of freedom command. Extended information about the model description can be found in (McGann & Arduino, 2010).

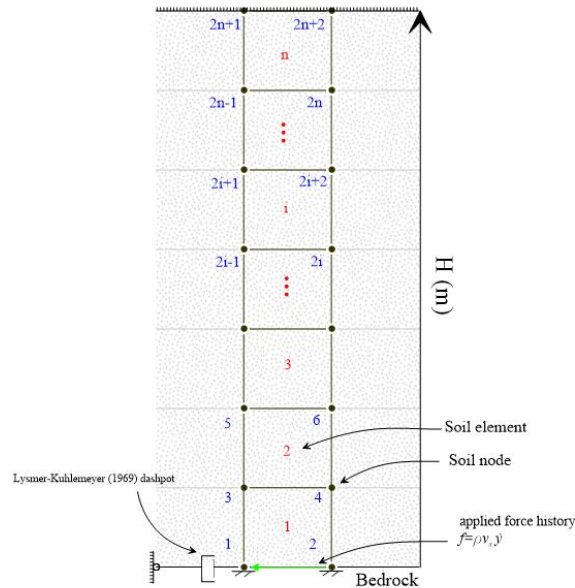


Figure 3. Visual representation of finite element site response model. (McGann & Arduino, 2010)

2.4.2 Soil Material Properties.

The mechanical behavior of the soil computed in the finite element model required shear wave velocity, Poisson ratio, and effective stress. The following subsection shows several inputs needed for the model and how these were obtained.

2.4.2.1 Poisson Ratio

Poisson's ratio (ν) allows the calculation of some elastic and mechanical parameters of the soil. Commonly, it is taken as constant for both unsaturated and saturated soils. Nevertheless, water content has a significant effect on this parameter on fine-grained soils. This means that Poisson's ratio has a relationship with the degree of saturation. Oh et al. propose an experimental relationship between Poisson's ratio (ν) and the degree of saturation (S_r) for fine-grained soils (Oh & Vanapalli, 2011). For the numerical model, Poisson's ratio was obtained for each layer using Oh's relationship.

2.4.2.2 Soil Shear Wave Velocity

Soil's shear wave velocity was computed using Eq (3), where (G) is the soil's shear modulus and (ρ) is the soil's density. Both properties were obtained using the rheometer and climate chamber tests performed in (Villacreses, Granados, Caicedo, Torres-Rodas, & Yépez, 2021) and (Lozada, Caicedo, & Thorel, 2019). The results were then interpolated for each suction value.

$$V_s = \sqrt{\frac{G}{\rho}} \quad (3)$$

From these values, Young (E) and bulk modulus (B) were obtained using Eq (4) and Eq (5) respectively.

$$E = 2G * (1 + \nu) \quad (4)$$

$$B = \frac{E}{(3*(1-2\nu))} \quad (5)$$

2.4.2.3 Effective stress.

Effective stress is important when computing the dynamic response of a soil deposit subjected to combined effects of confinement stress and suction pressure.

Equation (6) shows Bishop's approach to determining effective stress. This expression is explained in (Bishop, 1959) and will be used for this investigation.

$$\sigma' = (\sigma - u_a) + \chi(u_a - u_w) \quad (6)$$

Where σ' is the effective stress, $(\sigma - u_a)$ is the net stress, $(u_a - u_w)$ is the matric suction and χ is the effective stress parameter. For this investigation, the matric suction is assumed to be the same as the suction pressure. The effective stress parameter (χ) is a value related to the soil structure and it is used to describe the change in effective stress. Multiple attempts have tried to quantify χ theoretically and experimentally. One of

these approaches, shown in Eq (7) presents the best fit for an experimental relationship between χ and suction, proposed in (Khalili & Khabbaz, 1998).

$$\chi = \left[\frac{(u_a - u_w)}{(u_a - u_w)_b} \right]^{-0.55} \quad (7)$$

In this equation, $(u_a - u_w)_b$ is the suction for the air entry value, and this investigation adopts a value of 0.42MPa for this parameter (Villacreses, Caicedo, Caro, & Yépez, 2020). The equation shows that χ acquires a value of 0 for dry soils and 1 for saturated soils. This effective stress approach allowed the finite element model to determine the effective stresses values for different depths, saturation, and suction values in the soil deposit.

2.4.3 Seismic Motion.

The model applies an earthquake ground motion at the base of the soil column to analyze seismic wave propagation. In this investigation, three seismic accelerations obtained from Peer NGA strong motion database are used. Figure 4 shows the accelerograms and the Fast Fourier Transformation of the records. First, Figure 4a shows the 1989 Loma Prieta earthquake, from station Gilroy N°1 E-W. The record shows peak accelerations between seconds 3 to 5, indicating a maximum acceleration of 4.75 m/s², while the FFT demonstrates a predominant frequency of 2.65 Hz. Figure 4b shows the 1995 Kobe earthquake with an amplification two times the original signal. The signal was recorded in Kobe University station, located in the near field from the epicenter. The figure shows a maximum acceleration of 5.09 m/s² and a predominant frequency of 1.65 Hz. Finally, Figure 4c shows the 1989 Loma Prieta earthquake, from station Piedmont Jr High School, which is in the far-field from the epicenter. This signal is used with amplification of 5.8 times the original signal (Berkeley, n.d).

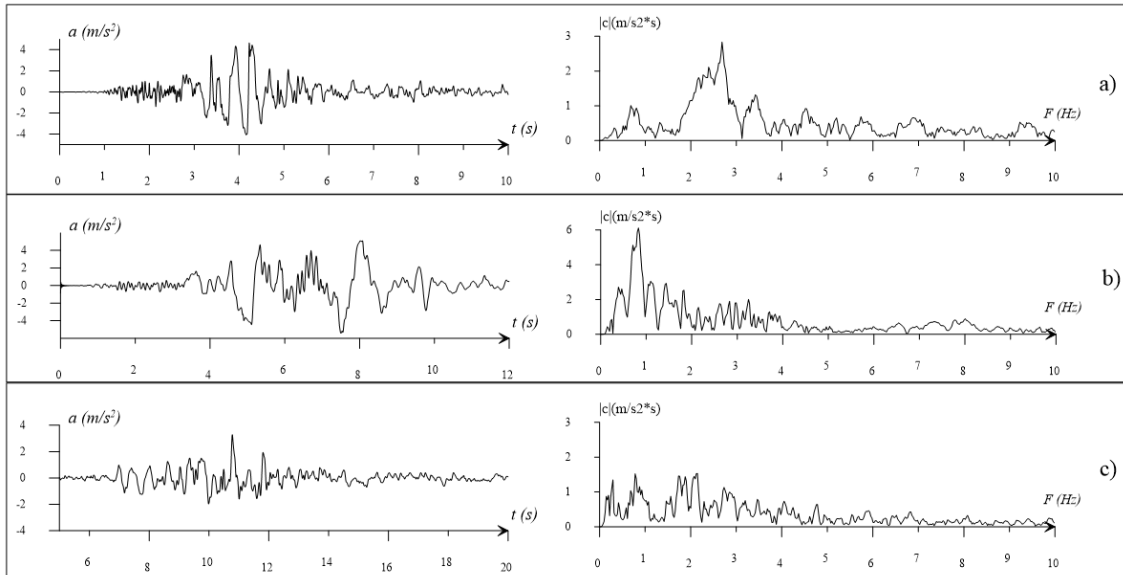


Figure 4. Applied ground motion acceleration and Fast Fourier Transform for a) 1989 Loma Prieta earthquake Gilroy N°1 E-W station b) amplified 1995 Kobe earthquake and c) amplified 1989 Loma Prieta earthquake Piedmont

3. Results and discussion.

In the next section, the results are discussed in the following order: first, results obtained in (Villacreses, Caicedo, Caro, & Yépez, 2020) and (Villacreses, Granados, Caicedo, Torres-Rodas, & Yépez, 2021) are analyzed to construct new relationships. Second, the results from the finite difference simulations were used to calculate the different water contents depending on the soil deposit depth. Finally, the seismic response is assessed through the finite element model using the three described motions. These results aim to understand the seismic response of a soil column under different water contents.

3.1 Material properties (climate chamber, rheometer).

Figure 2 shows the relationship obtained between suction pressure (ψ) and the degree of saturation (S_r). In this figure, it is possible to identify the increase in suction pressure following the drying path. Also, the figure demonstrates that the experimental results fit the model proposed by Fredlund & Xing in (Fredlund & Xing, 1994). Figure

5 illustrates the relationship between the degree of saturation (S_r) and soil's bulk density (γ_b). The figure shows that bulk density increases as a function of water content. For instance, Figure 5 shows that bulk density increases from 14.5 kN/m³ to 17 kN/m³ as the degree of saturation increases from 0.22 to 0.75.

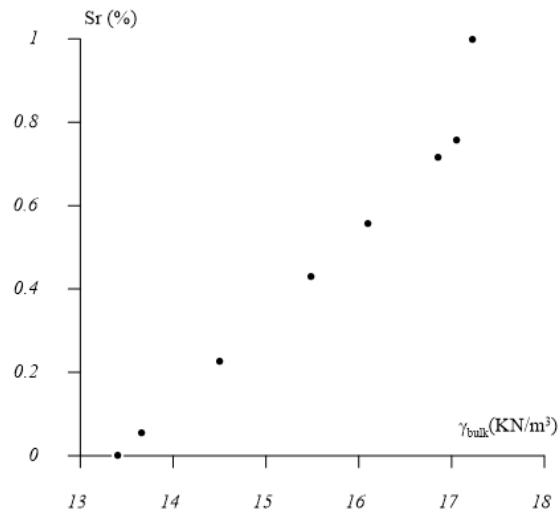


Figure 5. Degree of saturation as a function of bulk density.

Shear modulus is proportional to effective stress. Effective stress was calculated as a function of suction pressure and the soil depth using Eq.6 and Eq.7. Figure 6 illustrates the relationship between the shear modulus (G) and the effective stress (σ'). Undoubtedly, shear modulus increases as effective stress increase too. However, the figure shows that for effective stress values below the 550 KPa, there is no remarkable change in the shear modulus values.

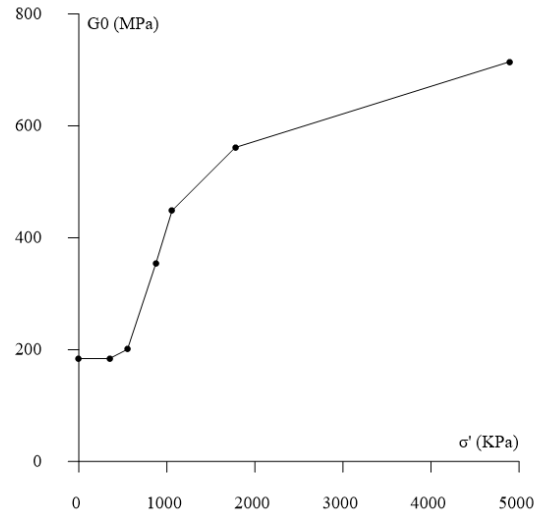


Figure 6. relationship between the shear modulus (G) and the effective stress (σ').

The finite element model used in this investigation defines yield surfaces based on shear modulus reduction curves. Figure 7 illustrates soil's modulus reduction curves (G/G_{max}) vs shear strain (ϵ) for multiple suction pressure values. The figure shows that for greater suction pressure values, the degradation of the shear modulus is less pronounced. Likewise, the figure shows that the shear modulus reduces as shear strain increases. For example, when the shear strain increases from 0.0001 to 0.001, most of the curves show degradation of almost 50%. The finite element model used these modulus reduction curves to run the response analysis. Intermediate values were linearly interpolated for different suction pressure values.

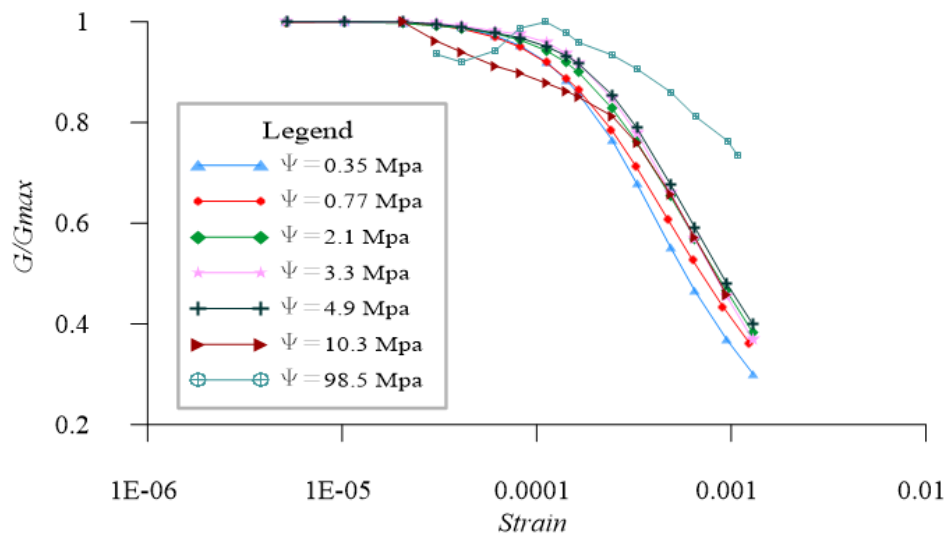


Figure 7. Modulus reduction curves for multiple suction pressure values

3.2 Finite-difference simulation (water table level and evaporation)

The finite-difference simulations were carried out in a thirty meters soil column, using different water table levels (i.e., 5, 15, and 25m). The simulation provides the relationship between the saturation degree (S_r), water pressure (U_w), and depth of soil deposit (H). Later, the numerical and experimental results were used to compute the bulk density (γ_b) for different depths along the soil strata (Villacreses, Caicedo, Caro, & Yépez, 2020), (Villacreses, Granados, Caicedo, Torres-Rodas, & Yépez, 2021). For this investigation, the numerical results of the evaporation model for 0, 600, and 87600 hours are used. These profiles are selected because they show a noteworthy difference in their results. Figure 8 shows the relationships obtained from the simulations, showing the variations in (S_r), (U_w) and (γ_b) along the soil depth. These results consider the different water table levels and the introduced climate conditions. For instance, it shows how bulk density rapidly changes as depth reaches water table level. Indeed, bulk density increases from 13.65 kN/m^3 to 17.22 kN/m^3 as the soil becomes saturated. The figure shows how the bulk density behaves like a straight line after the first 5 meters.

This is because after the first 5 meters the soil behaves as totally saturated. On the other hand, the figure illustrates that the degree of saturation slowly increases with depth until it reaches total saturation at the water table level. Also, the figure shows the difference in water pressure values depending on the water table level. For example, without carried evaporation, water pressure at the surface is -43.61 MPa when water table level is at a 5m depth and -239.61 MPa when water table level is at a 25m depth. These results show that water pressure is greater when the water table level is deeper. Water pressure does not have a significant difference in the first 600 hours of evaporation. Furthermore, 87600 hours of evaporation have a significant effect on water pressure values on the first meters of soil deposit.

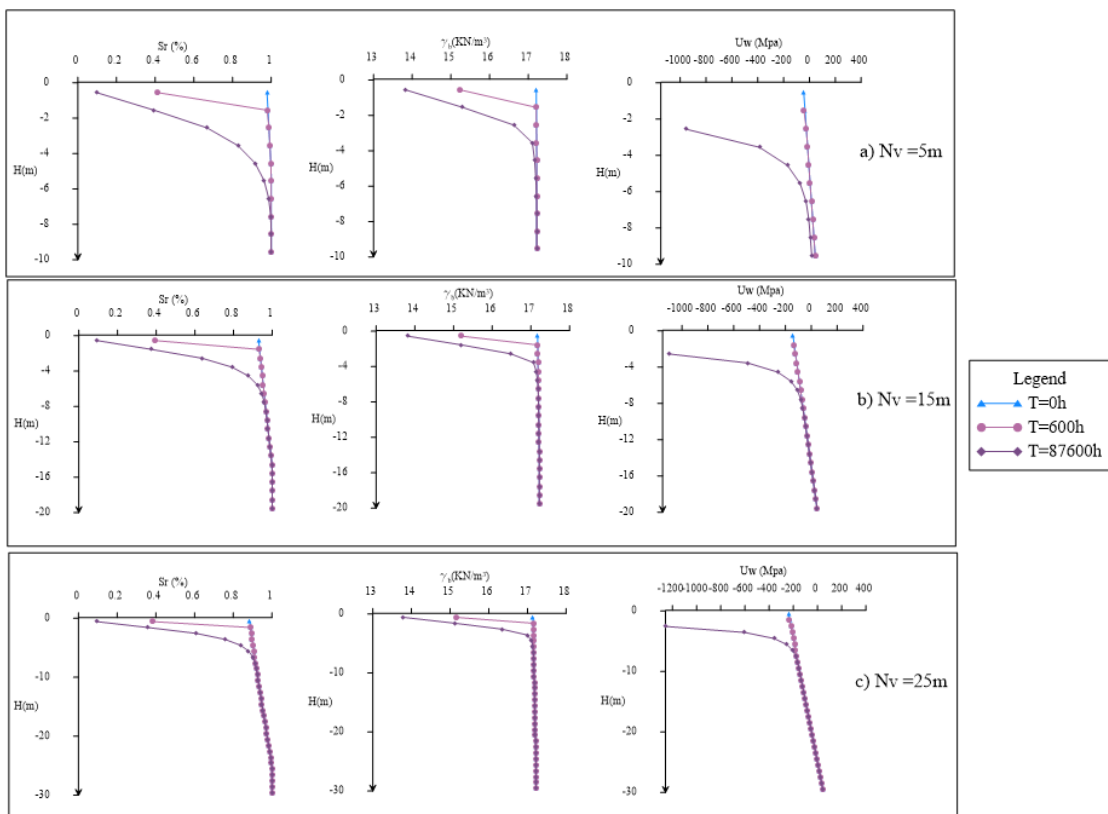


Figure 8. relationship between the degree of saturation (S_r), bulk density (γ_b), water pressure (U_w), and depth of soil deposit (H) for 0, 600, and 87600 hours of the evaporation process and water table levels of a)5m b)15m and c)25m

For seismic site effect, the most common mechanical properties are the shear modulus (G) and the shear wave velocity (V_s). Figure 9 illustrates the relationship between soil's mechanical properties and depth for different water table levels. Figure 9a shows the results for a water table level of 5m, Figure 9b for 15m, and Figure 9c for 25m. These relationships are presented for 0, 600, and 87600 hours of the evaporation process. As presented in Figure 9, both shear modulus and shear wave velocity do not have a remarkable change regarding water table level. The figure shows that the shear modulus remains virtually constant at a value of approximately 184.10 MPa after the first 5m. This is because the shear modulus is dependent on the effective stress and, after the first 5m, effective stress varies slightly. For instance, effective stress changes from 150 KPa and 350 KPa, which implies a variance in shear modulus of less than 0.11 MPa. Also, Figure 9 shows that the different water table levels do not produce a significant change in the shear modulus. However, shear modulus changes in the first meters of soil depth as a function of water evaporation. As an example, for a depth of 1.55 m, the shear modulus is almost 3 times bigger after an 87600-hour evaporation span. Figure 9a and 9b show that shear wave velocity has almost the same values for the deposits with water table levels of 5m and 15m. Nevertheless, Figure 9c shows that shear wave velocity does have a notable difference at the bottom of the deposit when the water table level is at 25m. As an example, for a depth of 20m and no carried evaporation, shear wave velocity is 323.82 m/s for water table level of 5m and 326.81 m/s for water table level 25m. These results change for a depth of 29.5m since shear wave velocity is 323.84 m/s for water table level of 5m and 331.86 m/s for water table level of 25m.

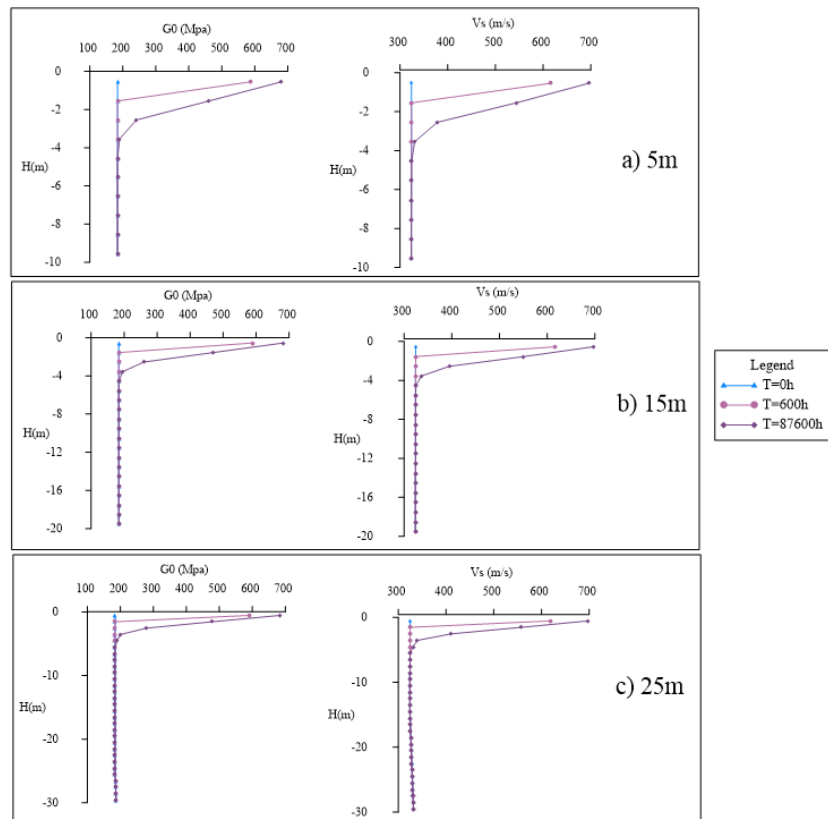


Figure 9. relationship between a) shear modulus and depth for different water table levels and b) shear wave velocity and depth for different water table levels for 0, 600, and 87600 hours of the evaporation process

3.3 Seismic response

The previous results showed the difference in the mechanical properties of soil according to the depth, water table levels, and evaporation conditions of the deposit. Similarly, the results showed the impact that suction pressure and degree of saturation have on the soil's mechanical properties. Once obtained these results, the finite element model introduces a ground motion acceleration at the base of the deposit. The unidimensional wave propagation allows the seismic response at the top of the soil deposit to be computed. In this manner, the seismic records presented in Figure 4 are introduced in the model. Furthermore, the period of the soil deposit was estimated. This value ranges between 0.35 and 0.37 seconds depending on the water table level and the climate condition imposed. Additionally, the surface response accelerograms were used to compute acceleration response spectrums for different simple oscillators periods.

Figure 10 illustrates the response acceleration spectrum at the top of the soil column obtained from introducing the 1995 Kobe earthquake signal in the model. Also, the figure shows the different outcomes considering distinct water table levels (i.e., 5, 15, 25m) and regarding 0 and 10 years of evaporation. The following analyses will focus on the effects of water table level and climate conditions on the seismic response. Starting with the effects of climate conditions, Figure 10 shows that the evaporation changes do not have a significant effect on the seismic response of the soil deposit. For example, the response spectrum of the 5m water table shows that the maximum acceleration for the 0 years is 18.39 m/s^2 whereas for the 10th year is 18.31 m/s^2 . Thus, a 10-year evaporation span produces a percentual difference of 0.4% in the maximum acceleration response. Analyzing the effects of the water table level, Figure 10 shows that the water table modifies the response of the soil deposit. Notably, the results reveal that the acceleration increase as the depth of the water table level does. As an example, when the period of the oscillator is close to the period of the deposit, the bedrock acceleration in the spectrum is 11.45 m/s^2 . This value is amplified to 17.98 m/s^2 when the water table level is at 5m and amplified to 18.66 m/s^2 when the water table level is at 25m. Therefore, the results show that the acceleration response has a percentual increase of 3.78% when the water table level is closest to the bottom. This amplification can be explained by analyzing the Fast Forward Transform of the signal shown in Figure 4b. The figure shows that the frequency content of the signal ranges from 0.2 Hz and 3.2 Hz. Thus, for values close to the natural frequency of the deposit, there is significant frequency content in the spectrum, which allows the amplification to take place.

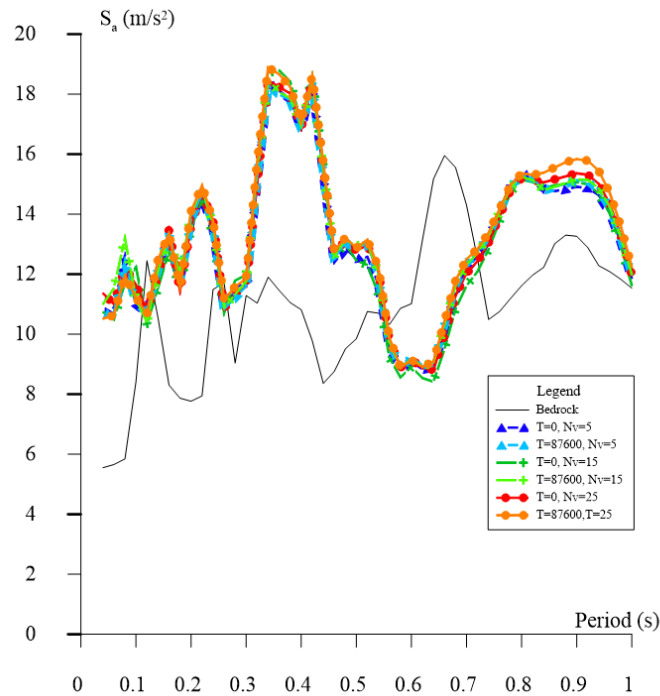


Figure 10. 1995 Kobe earthquake acceleration response spectrum at top of the deposit for different water table levels (i.e., 5, 15, 25m) and exposed to 0 and 87600 hours of evaporation

Figure 11 shows the response acceleration spectrum obtained from introducing the Loma Prieta - Piedmont station signal in the model. The figure shows similar results to those obtained previously with the Kobe signal. Starting with the effects of climate conditions, Figure 11 shows that the evaporation process in this deposit does not have a remarkable difference in the acceleration response of the signal. For instance, using an oscillator period of 0.36 seconds and a water table level of 5 m, the acceleration response is 8.34 m/s^2 when there is no evaporation and 8.57 m/s^2 for a 10-year evaporation span. These results show that, for this period, the climate conditions had a percentual difference of 2.7% in the acceleration response. Analyzing the effects of the water table level, Figure 11 shows that the water table modifies the response of the soil deposit. Since climate effects do not affect the response, the following analyses will consider no evaporation. The figure shows that, for a water table level of 5m, and a period of 0.34s, the acceleration response is 8.46 m/s^2 whereas for a water table level of

25m the acceleration response is 9.15 m/s^2 . These results show that, for this period, the water table level produce a percentual difference of 8.15% in the acceleration response. Also, the results show that, for this period, the deposit will amplify the bedrock acceleration 25.85% its value when the water table level is at 25m. To sum up, Figure 11 shows that when the oscillator period is close to one of the deposits, the acceleration spectrum at the surface is amplified. Additionally, this amplification is greater when the water table level is deeper. The Fast Forward Transform of the signal in Figure 4c shows that the frequency content of the motion is relatively uniform. The amplification of the signal takes place since there is significant frequency content for values close to the natural frequency of the deposit.

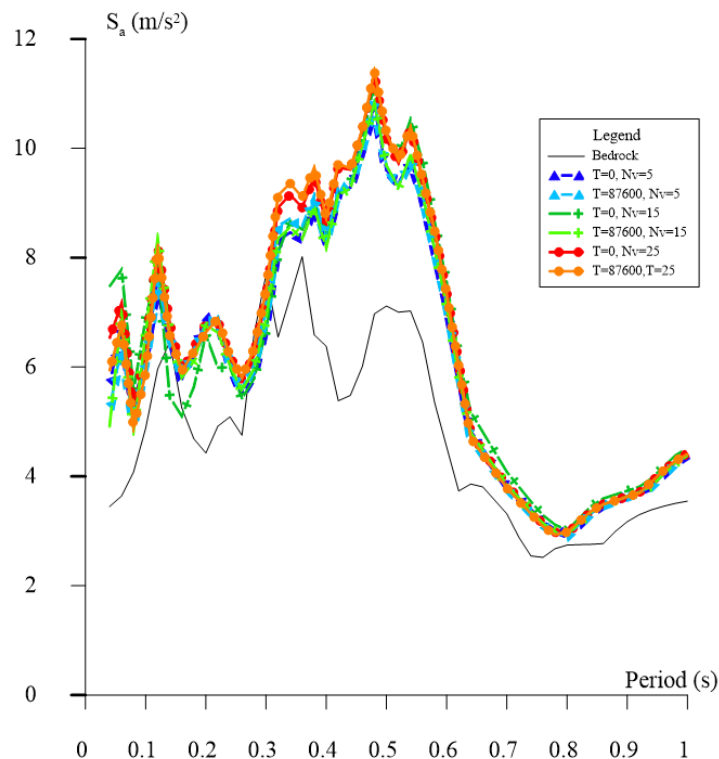


Figure 11. 1989 Loma Prieta (Piedmont station) acceleration response spectrum at top of the deposit for different water table levels (i.e., 5, 15, 25m) and exposed to 0 and 87600 hours of evaporation

The acceleration response spectrum obtained from introducing the Loma Prieta Gilroy station signal in the model is shown in Figure 12. Principally, the figure shows a

remarkable difference in the response in comparison to the previously analyzed signals. This is because Figure 12 shows a strong reduction in the acceleration response at the top of the deposit. First, the effects of the evaporation process in the response will be analyzed. The figure shows that the climate effects on the deposit do not have a noteworthy effect on the response. For instance, for a water table level of 5 m, the maximum acceleration response is 13.10 m/s^2 for 0 hours of evaporation and 13.10 m/s^2 for a 10-year evaporation span. Analyzing the effect of the water table level, the results show that the response is slightly different between the various water table levels. For example, for a water table level of 5 m, and an oscillator period of 0.36 seconds the acceleration spectrum de-amplifies from 19.05 m/s^2 to 12.74 m/s^2 . On the other hand, this value de-amplifies to 13.22 m/s^2 when the water table level is 25 m. This means that when the deposit is dryer, the acceleration response is 3.76% higher than when the deposit is saturated. Figure 4a shows the Fast Forward Transform of the signal. The figure illustrates that the frequency content ranges from 2 Hz and 3 Hz, with a clear peak of 2.7 Hz. On the other hand, for values close to the natural frequency of the deposit, there is low frequency content in comparison to the observed peak. In this manner, the de-amplification in the spectrum can be explained as a function of the decay in the frequency content. The figure shows that the seismic response does not only depends on the mechanical properties of the deposit but also depends on the frequency content of the signal.

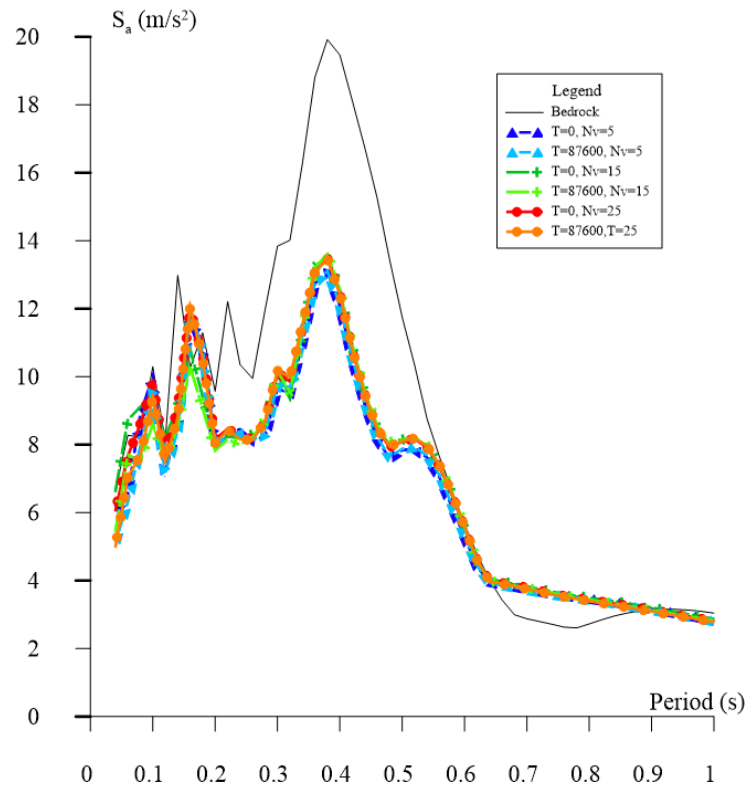


Figure 12. 1989 Loma Prieta (Gilroy N°1 E-W) acceleration response spectrum at top of the deposit for different water table levels (i.e., 5, 15, 25m) and exposed to 0 and 87600 hours of evaporation

Conclusions

This work presents the seismic response analysis of a soil column influenced by different water table levels (i.e., 5m, 15m, 25m) and subjected to periods of evaporation (i.e., 0s, 600s, 87600s). To achieve this objective, a finite difference model presented in (Villacreses, Granados, Caicedo, Torres-Rodas, & Yépez, 2021) was used to simulate soil drying under climate conditions. Then, a finite element model presented in (McGann & Arduino, 2010) was modified to obtain the seismic response at the top of the soil column. The finite-difference model showed that, for the studied soil, the environmental interaction does not have a remarkable change along with the soil depth after the first 5 meters. Likewise, the finite element model showed that there is no remarkable difference in the seismic response of the soil column after being exposed to climate conditions. Nevertheless, the results suggest that the water table level does have

a noteworthy effect on the dynamic response of the earth structure. The results showed that the deposit in dryer conditions had a greater acceleration response than the more saturated deposits. Finally, the results from the seismic response showed that some records are amplified, and others are reduced by the soil deposit. In this manner, this research opens new possibilities in the research field, in which more seismic records should be analyzed, epicenter proximity should be considered, and fundamental period degradation should be profoundly analyzed. Also, this investigation could be replicated using limes, sands, and different types of soils. This study showed that these conditions can influence the mechanical and dynamical behavior of soil deposits and further investigations must be done since these aspects can impact the construction, reinforcement, and maintenance of soil structures in the future.

References

- Berkeley, U. (n.d). *PEER Strong Ground Motion Databases. Pacific Earthquake Engineering Research Center*. Retrieved november 2021, from <https://peer.berkeley.edu/peer-strong-ground-motion-databases>
- Bishop, A. W. (1959). The principle of effective stress. *Teknisk ukeblad*, 39, 859–863.
- Fredlund, D. G., & Xing, A. (1994). Equations for the soil-water characteristic curve. *Canadian geotechnical journal*, 31, 521–532.
- Khalili, N., & Khabbaz, M. H. (1998). A unique relationship for χ for the determination of the shear strength of unsaturated soils. *Geotechnique*, 48, 681–687.
- Leong, E.-C., Tripathy, S., & Rahardjo, H. (2003). Total suction measurement of unsaturated soils with a device using the chilled-mirror dew-point technique. *Geotechnique*, 53, 173–182.
- Lozada, C., Caicedo, B., & Thorel, L. (2019). A new climatic chamber for studying soil–atmosphere interaction in physical models. *International Journal of Physical Modelling in Geotechnics*, 19, 286–304.
- Lysmer, J., & Kuhlemeyer, R. L. (1969). Finite dynamic model for infinite media. *Journal of the Engineering Mechanics Division*, 95, 859–877.
- McGann, C., & Arduino, P. (2010). Site response analysis of a layered soil column (total stress analysis). *Opensees Example Wiki. University of Washington*.
- MIDUVI. (2014). Norma Ecuatoriana de la Construcción. Geotécnia y Cimentaciones.
- Oh, W. T., & Vanapalli, S. K. (2011). Relationship between Poisson’s ratio and soil suction for unsaturated soils. *Proc., 5th Asia-Pacific Conf. on Unsaturated Soils*, (págs. 239–245).
- Sánchez Sesma, F. J., Rodríguez Zúñiga, J. L., Pérez Rocha, L. E., Cuevas, A., & Suarez, M. (1992). The seismic response of shallow alluvial valleys using a simplified model. En *Memoria* (págs. 237–44).
- Villacreses, J. P., Caicedo, B., Caro, S., & Yépez, F. (2020). A novel procedure to determine shear dynamic modulus and damping ratio for partial saturated compacted fine-grained soils. *Soil Dynamics and Earthquake Engineering*, 131, 106029.
- Villacreses, J. P., Granados, J., Caicedo, B., Torres-Rodas, P., & Yépez, F. (2021). Seismic and hydromechanical performance of rammed earth walls under changing environmental conditions. *Construction and Building Materials*, 300, 124331.

